Hemispheric Insolation Forcing of the Indian Ocean and Asian Monsoon: Local versus Remote Impacts*

XIAODONG LIU
SKLLQG, Institute of Earth Environment, Chinese Academy of Sciences, Xi'an, China

ZHENGYU LIU AND JOHN E. KUTZBACH
Center for Climatic Research, University of Wisconsin—Madison, Madison, Wisconsin

STEVEN C. CLEMENS AND WARREN L. PRELL
Geological Sciences, Brown University, Providence, Rhode Island

(Manuscript received 13 September 2005, in final form 21 March 2006)

ABSTRACT

Insolation forcing related to the earth's orbital parameters is known to play an important role in regulating variations of the South Asian monsoon on geological time scales. The influence of insolation forcing on the Indian Ocean and Asian monsoon is studied in this paper by isolating the Northern and Southern Hemispheric insolation changes in several numerical experiments with a coupled ocean–atmosphere model. The focus is on the response of South Asian summer rainfall (monsoon strength) with emphasis on impacts of the local versus remote forcing and possible mechanisms. The model results show that both Northern Hemisphere (NH) and Southern Hemisphere (SH) summer insolation changes affect the Indian Ocean and Asian monsoon as a local forcing (in the same hemisphere), but only the SH changes result in remote (in the other hemisphere) forcing. The NH insolation change has a local and immediate impact on NH summer monsoons from North Africa to South and East Asia, while the SH insolation change has a remote and seasonal-scale delayed effect on the South Asian summer monsoon rainfall. When the SH insolation is increased from December to April, the sea surface temperature (SST) in the southern tropical Indian Ocean remains high from January to July. The increased SST produces more atmospheric precipitable water over the southern tropical Indian Ocean by promoting evaporation from the ocean. The enhanced precipitable water over the southern Indian Ocean is transported northward to the South Asian monsoon region by the lower-tropospheric mean cross-equatorial flows with the onset of the Asian monsoon increasing precipitable water over South Asia, eventually leading to the increase of Indian summer monsoon precipitation. Thus, these model experiments, while idealized and not fully representing actual orbitally forced insolation changes, confirm the broadscale response of northern monsoons to NH summer insolation increases and also illustrate how SH summer insolation increases can have a delayed influence on the Indian summer monsoon.

1. Introduction

Changes in solar radiation significantly influence climate change at various time scales (Rind 2002). On time scales of 10^3 to 10^5 years variations in the pattern of incoming solar radiation mainly result from secular changes in the earth's orbit around the sun, namely the orbital cycles of eccentricity (~100 kyr), obliquity (~41 kyr), and the precession of the equinoxes (~23 kyr) (Berger and Loutre 1991). Insolation change related to the earth's orbital forcing plays a primary role in driving quasi-periodic variations in climate at geological time scales (Milankovitch astronomical theory of paleoclimates; Ruddiman 2001). Both observational and modeling studies show that the Asian monsoon has distinct responses to changes in insolation (Ruddiman 2001). Moreover, the Asian monsoon variability in turn may modulate global or Northern Hemisphere (NH) climate changes (Kudrass et al. 2001; Leuschner and Sirocko 2003).

Geological archives have been used extensively to monitor Asian monsoon change at geological time

* Center for Climate Research Contribution Number 891.

Corresponding author address: Dr. Xiaodong Liu, Institute of Earth Environment, Chinese Academy of Sciences, 10 Fenghui South Road, Hi-Tech Zone, P.O. Box 17, Xi'An 710075, China.
E-mail: liuxd@loess.llqg.ac.cn

scales. Prell (1984) initiated orbital-scale studies of the Indian summer monsoon within the context of time series analysis clearly documenting orbital-driven monsoonal variability. Prell used percent variations of the planktonic foraminifera *Globigerina bulloides* from the northern Arabian Sea as a proxy for upwelling driven by changes in the Indian southwest monsoonal winds (Prell 1984; Prell and Van Campo 1986; Clemens et al. 1991). Recently, Clemens and Prell (2003) assessed orbital-scale monsoonal variability over the past 350 ka using five different proxies (physical, chemical, isotopic, and biological). Each of the five proxy records is independently linked to summer monsoon circulation strength within the atmospheric and oceanographic systems. These findings are discussed further below.

Additional studies have focused on the orbital-scale variability of the East Asian monsoon based on terrestrial records. For example, an East Asian winter monsoon proxy reconstructed from the Chinese loess plateau shows climatic variations at orbital periods over the past 2.5 Myr (Ding et al. 1994; Liu et al. 1999). Using a pollen record of *Cryptomeria japonica* from the North Pacific off Japan, Morley and Heusser (1997) demonstrated that the East Asian summer monsoon is coherent with orbital variability. Geochemical records from the South China Sea also indicate clear astronomical forcing of the East Asian monsoon (Wehausen and Brumsack 2002).

With the abundant geological evidence for the insolation–monsoon connection, the driving mechanisms and influential processes related to orbital forcing have received increasing attention. The 23- and 41-kyr periodic components of the climate change are usually regarded as a linear response to the orbital forcing with appropriate lags (Imbrie et al. 1992). Clemens, Prell, and colleagues (Prell 1984; Clemens et al. 1991; Clemens et al. 1996; Clemens and Prell 2003) have documented that the Asian summer monsoon is sensitive to orbital forcing at the obliquity and precession periods (41 and 23 kyr, respectively) as well as to the extent of NH glaciation, at least within the precession band. Over the past 350 kyr, they find that precession-band maxima in monsoon strength occur about 8 kyr after maxima in precessional summer radiation over Asia (21 June perihelion) and ~3 kyr after minimum glacial conditions. Over the obliquity band, they find that monsoon maxima occur simultaneously with maxima in NH summer radiation (obliquity maximum) and ~7 kyr before minimum glacial conditions. These phase relationships cannot be interpreted within the context of a simple linear response to increased NH summer insolation and decreased glacial conditions. Instead, they suggest that the timing of maximum monsoon strength within each precession or obliquity cycle is also influenced by the timing of maximum latent heat export from the southern subtripical Indian Ocean. Clemens and Press (2003) make the case that maximum latent heat export takes place at times of maximum obliquity and precession (21 December perihelion), accounting for 1) the in-phase relationship between summer monsoon strength and NH obliquity insolation forcing, 2) the ~8-kyr phase lag between summer monsoon strength and NH precessional insolation forcing, and 3) the observation that the summer monsoon has approximately equal amounts of variance in the obliquity and precession bands in spite of the fact that insolation is dominated by precession.

A large number of modeling studies have found orbital signals in the South Asian monsoonal systems. Most of them strongly emphasize the direct link between increased NH summer insolation and strengthened Indian and Asian monsoons (e.g., Kutzbach 1981; Kutzbach and Guetter 1986; Prell and Kutzbach 1987; de Noblet et al. 1996). For example, Prell and Kutzbach (1987) conducted a series of general circulation model (GCM) sensitivity tests and found that the monsoon strengthens with increasing NH summer insolation and weakens with increasing glacial boundary condition forcing. In recent years, ocean–atmosphere coupled models have been used to investigate the response of the Asian monsoon to orbital forcing and the internal feedback mechanisms that may amplify or dampen the initial solar forcing (e.g., Hewitt and Mitchell 1998; Braconnot et al. 2002; Liu et al. 2004). Using a coupled ocean–atmosphere GCM, for example, Liu et al. (2004) investigated the responses of the summer monsoon systems of all the major continents to mid-Holocene insolation forcing and oceanic feedback. These results indicate that the climatic response to orbital forcing can be amplified or damped by ocean feedbacks (Kutzbach and Liu 1997; Khodri et al. 2001; Philander and Fedorov 2003).

The Indian Ocean, including the southern tropical Indian Ocean, provides a major moisture source for the South Asian summer monsoon (Meehl 1997; Wajsowicz and Schopf 2001). Nearly 90% of the water vapor available to precipitate over India during the southwest monsoon results from the annual mean evaporation field (Wajsowicz and Schopf 2001). The sea surface temperature (SST) in the Indian Ocean associated with evaporation and water vapor transport has a significant impact on the Asian monsoon (Zhu and Houghton 1996; Meehl and Arblaster 2002). Results from numerical experiments show that increased moisture from the warmer Indian Ocean can result in greater Asian monsoon precipitation (Meehl and Arblaster 2003). There-

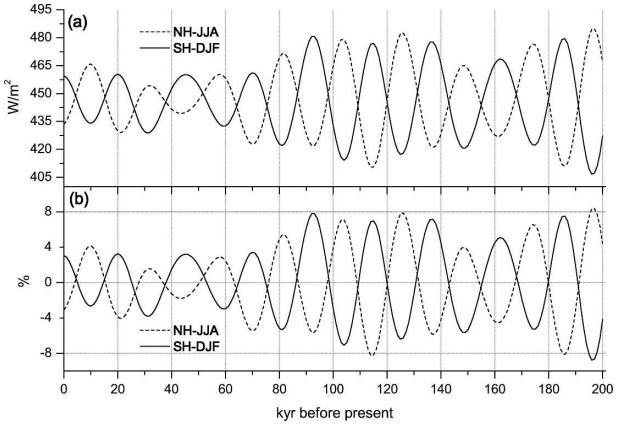

FIG. 1. (a) Area-weight-averaged SH DJF and NH JJA mean insolation and (b) their percentage variations with respect to the multiyear mean values during the past 200 000 yr [the insolation data from Berger and Loutre (1991)].

fore, the computed SST of the Indian Ocean is critical in correctly simulating atmospheric responses and physical processes related to orbital forcing in a coupled model (Clemens and Oglesby 1992).

Concerning the response of the South Asian monsoon to orbital forcing, although many investigations have been performed, none directly address the physical mechanism responsible for the observed phase relationships of an approximate 8-kyr lag between monsoon circulation maxima and NH summer insolation maxima at the precession band and the zero phase at the obliquity band, as Clemens et al. (1991) find from the geological record. Is the timing of latent heat export from the southern subtropical Indian Ocean responsible, as Clemens et al. (1991) and Clemens and Prell (2003) suggest?

Intuitively, monsoonal climate variability in low-latitude regions should be dominated by precessional variance, given the dominance of precessional insolation at low latitudes (Prell and Kutzbach 1987). However, Clemens and Prell (2003) find that summer monsoon variance as inferred from Arabian Sea proxies is equally distributed between the precession and obliquity bands. While the insolation signal associated with obliquity is hemispherically symmetric, the precession insolation forcing is hemispherically asymmetric. Taking Fig. 1 as an example that shows SH December–February (DJF) and NH June–August (JJA) mean insolation during the past 200 000 yr, we can see that warm NH and SH summers occur 180°, or about 11.5 kyr out of phase with one another at the precession band (Kutzbach and Guetter 1986; Clemens 1999). The maximum amplitude of the hemispheric insolation variations may reach ~8%, a percentage change with respect to the past 200-kyr mean values (Fig. 1b). Clemens and Prell (2003) suggest that warmer SH summers (NH winters) precondition the southern subtropical Indian Ocean to release greater amounts of latent heat during the following Northern Hemisphere summer monsoon. The phase of the monsoon proxies is consistent with this mechanism at both the precession and obliquity bands (after allowing for the influence of NH insolation at the precession band being modulated and phase-lagged by ice-volume effects), possibly accounting for the equal amounts of variance in both bands; the sensible and latent heat mechanisms are in phase at the obliquity band and out of phase at the precession band.

To address the latent heat mechanism, we will examine the effects of changes in SH and NH summertime solar radiation on Indian Ocean and Asian monsoon variability with a focus on the local (from the same hemisphere) versus remote (from the other hemisphere) impacts using a coupled ocean–atmosphere model. To test the hypothesis that latent heat transport from the southern subtropical Indian Ocean is essential in establishing timing of strong summer monsoons, we examine the influence of the SH summer solar radiation on the following South Asian summer monsoon. This is the first attempt, in paleomonsoon modeling, to identify the possible distinct role of insolation forcing from the two hemispheres, and therefore we use idealized (nonorbital) forcing to isolate the effect of single-hemisphere forcing in summer only. The model and experimental setup used for the simulations are described in section 2. Section 3 presents the primary results concerning hemispheric insolation influences on precipitation, atmospheric precipitable water, SST circulation, and moisture transport, as well as the comparison of the local versus remote impacts. We conclude with a summary and discussion.

2. Model and experimental design

The model we used is the Fast Ocean–Atmosphere Model (FOAM), version 1.5 (Jacob 1997). FOAM is a fully coupled ocean–atmosphere GCM without flux adjustment. The atmospheric component of FOAM is a fully parallel version of the National Center for Atmospheric Research (NCAR) Community Climate Model (CCM) version 2, in which the atmospheric physics are replaced by those of NCAR CCM version 3.6. The spectral atmosphere model has an R15 resolution (equivalent grid spacing about 4.4° latitude × 7.5° longitude) with 18 vertical levels. The ocean component model was developed from the Geophysical Fluid Dynamics Laboratory (GFDL) Modular Ocean Model (MOM), with a horizontal resolution of 1.4° in latitude, 2.8° in longitude, and 32 layers in the vertical. FOAM does not include the land surface model that was intro-

duced with CCM 3.6; instead, the Lund–Potsdam–Jena dynamic global vegetation model (Sitch et al. 2003) has been coupled to the present version of FOAM (Gallimore et al. 2005). The horizontal resolution of the vegetation model used here is the same as that of the ocean model. In addition, FOAM uses NCAR's thermodynamical sea ice component model. All components of FOAM are linked to each other through a coupler to carry out the exchange of fluxes between them (sensible and latent heat, momentum, etc.).

The quality of the simulated climate with FOAM compares well with higher-resolution models. Without flux correction, FOAM has shown a good performance in simulating the observed tropical climatology (Jacob 1997), paleoclimates (Liu et al. 2000; Liu et al. 2004), and long-term natural variability of the ocean–atmosphere system in the Pacific (Wu and Liu 2003; Liu and Wu 2004) and Atlantic (Wu and Liu 2005). Here, we will focus on responses of the Indian Ocean and Asian monsoon to the insolation forcing.

We first performed a modern control simulation (experiment CTL). The CTL run is integrated for 100 yr, starting from another long control simulation, and it uses modern boundary conditions, including present-day topography, insolation, and preindustrial CO_2 concentration of 280 ppm. We then performed two parallel 100-yr sensitivity experiments, which are designed specifically to cleanly isolate the effect of the local hemispheric insolation forcing from the remote hemispheric insolation forcing on the Asian monsoon. The first experiment (experiment NH) is identical to the experiment CTL except that the NH insolation is increased by 7.5% from May to September of each year. The May–September average insolation for the NH is ~32 W m^{-2} higher in experiment NH than that in experiment CTL, while the insolation for the SH remains unchanged (Fig. 2a). The second experiment (experiment SH) is complementary to the first, with the insolation increased 8% (~32 W m^{-2} on average) in the SH from December to April relative to experiment CTL (Fig. 2b). [The SH insolation is increased by 8% in experiment SH because the maximum amplitude of the hemispheric insolation variations is close to this percentage value (see Fig. 1b). Because of the larger mean insolation in NH summer (JJA) than that in SH summer (DJF), however, the percentage increase in NH insolation is set as 7.5% in experiment NH, slightly less than in experiment SH, in order to keep the same absolute increment of insolation (~32 W m^{-2}) in both experiments.] Since each experiment reaches a quasi-equilibrium state in the surface climate after 70 yr of integration, we will analyze the last 30 yr of simulation

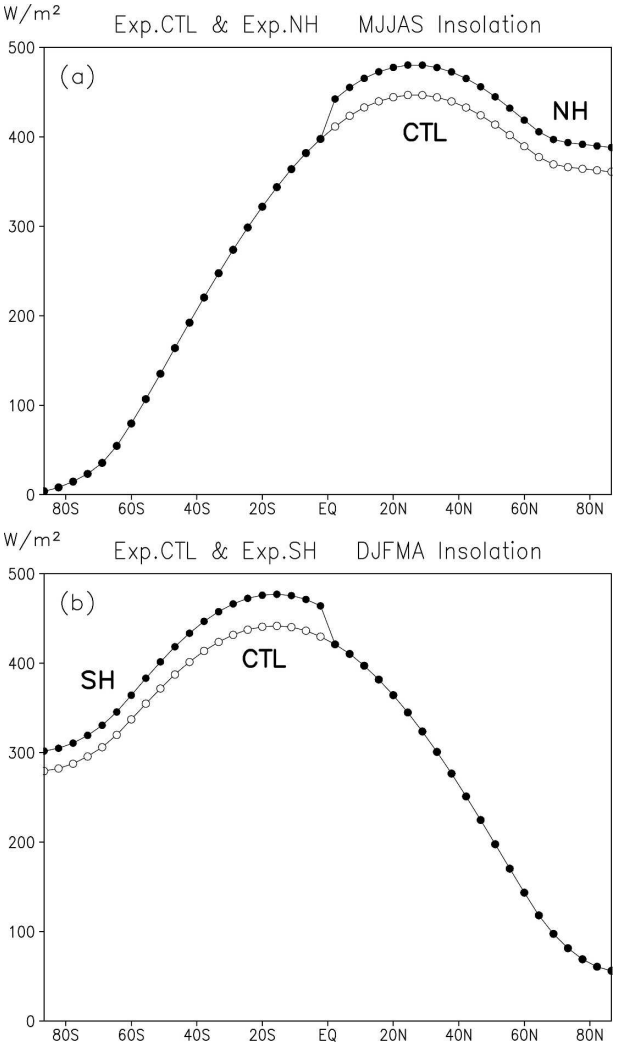

FIG. 2. (a) Insolation averaged for May to September in experiments CTL and NH and (b) that averaged for December to April in experiments CTL and SH, as a function of latitude.

in each experiment. The specifically designed insolation forcings in the two sensitivity experiments enable us to cleanly separate the local (from the same hemisphere) versus remote (from the opposite hemisphere) insolation forcing: in experiment NH, the NH anomalous insolation forcing acts as a local forcing on the Asian monsoon, but a remote forcing to the Southern Hemisphere Indian Ocean; in experiment SH, the SH anomalous insolation forcing acts as the local forcing to the Southern Hemisphere Indian Ocean, but a remote forcing to the Asian monsoon. This type of idealized forcing, although it differs from true orbitally caused insolation forcing by omitting full seasonal effects and full latitudinal effects that extend across the equator, has the advantage of cleanly separating the local versus remote forcing and therefore is useful for our under-

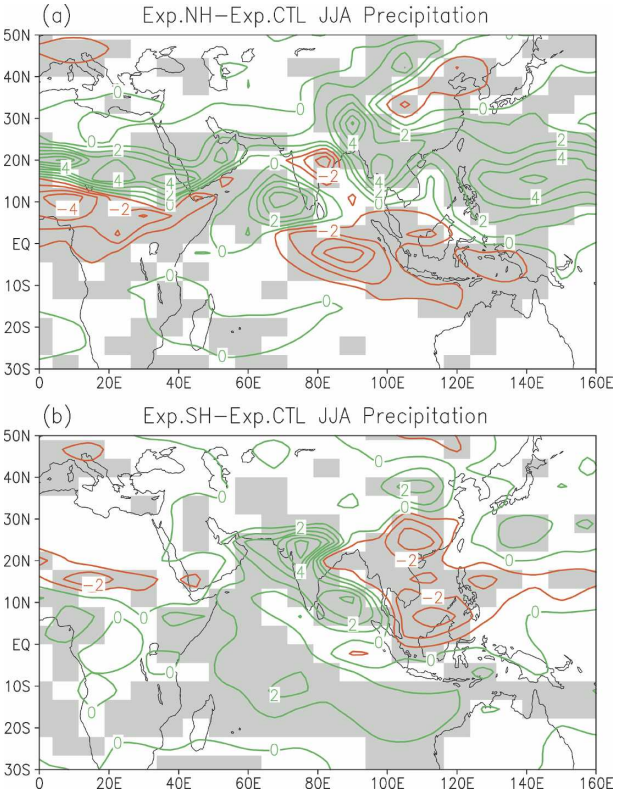

FIG. 3. (a) JJA mean precipitation rate difference between experiments NH and CTL and (b) that between experiments SH and CTL. Unit is mm day^{-1}. The shaded areas are statistically significant at the 99% confidence level or higher, according to the Student's *t* test.

standing of the remote forcing impact on the Asian monsoon.

3. Results

a. Precipitation

Enhancement of both NH and SH summer insolation produces increased precipitation for particular regions of the northern summer monsoon. The JJA precipitation difference between experiments NH and CTL (Fig. 3a) indicates significantly increased precipitation over the sub-Sahara part of North Africa, the eastern Arabian Sea, the southern slope of the Tibetan Plateau, parts of Southeast and East Asia, and the North Pacific when NH insolation is increased from May to September. In contrast, stronger SH insolation during December to April yields increased JJA precipitation over India, parts of East Asia, the Bay of Bengal, and the northern and southern tropical Indian Ocean but less precipitation over North Africa, the South China Sea, and southern China (Fig. 3b). Thus, most NH monsoon lands have a direct response to NH summer insolation while India in particular has a delayed response to the preceding (December–April) SH insolation. In other words, NH insolation can be regarded as a local, immediate forcing of the North African and Asian summer monsoons (except for part of India) whereas SH insolation serves as a remote forcing of the Indian summer monsoon with time lag of one of two seasons. This result shows that the change in SH summer insolation can influence the following boreal summer monsoon, particularly over India, as Clemens et al. (1991) and Clemens and Prell (2003) suggest. However, the mechanism is not immediately clear. Generally speaking, two mechanisms may be responsible for variations in Asian monsoon rainfall: change in atmospheric moisture content that includes water vapor coming from the southern Indian Ocean and/or change in the monsoon circulation related to large-scale land–sea thermal contrast. Of course, the result may also be due to a combination of these two mechanisms.

In the following sections, we will analyze the total water vapor, moisture transport, and monsoonal wind fields to further explore the influence of SH summer insolation change on boreal summer monsoon rainfall. As a comparison, we will also examine the impact of NH insolation to illustrate the asymmetry of hemispheric insolation forcing.

b. SST and total precipitable water

Change in SST is important in the energy balance and the interhemispheric heat exchange over the Asian continent and Indian Ocean in a coupled ocean–atmosphere system (Wang et al. 2003b; Clemens and Oglesby 1992). Our experiments indicate that SST in the Indian Ocean and western Pacific increases in response to enhanced hemispheric insolation (Fig. 4). When the NH insolation is strengthened from May to September, the SST in the North Pacific and Indian Oceans, and surface air temperature over the Eurasian continent increase in all four seasons, especially in JJA (Fig. 4e) and September–November (SON; Fig. 4g). When the SH insolation is intensified from December to April, however, the SST increases in the southern Indian Ocean all year-round. The strongest SST increase in the southern Indian Ocean occurs in boreal spring, March–May (MAM), before the onset of the Asian summer monsoon (Fig. 4d). The MAM SST is 3°C higher in the central part of the southern Indian Ocean in experiment SH than that in experiment CTL. The SST response lags the insolation forcing by 2–3 months (Braconnot et al. 2000; Khodri et al. 2001). The higher SST likely leads to increased evaporation from the ocean and increased atmospheric moisture.

The spatiotemporal pattern of total precipitable water (TPW) over the Indian Ocean and nearby regions is

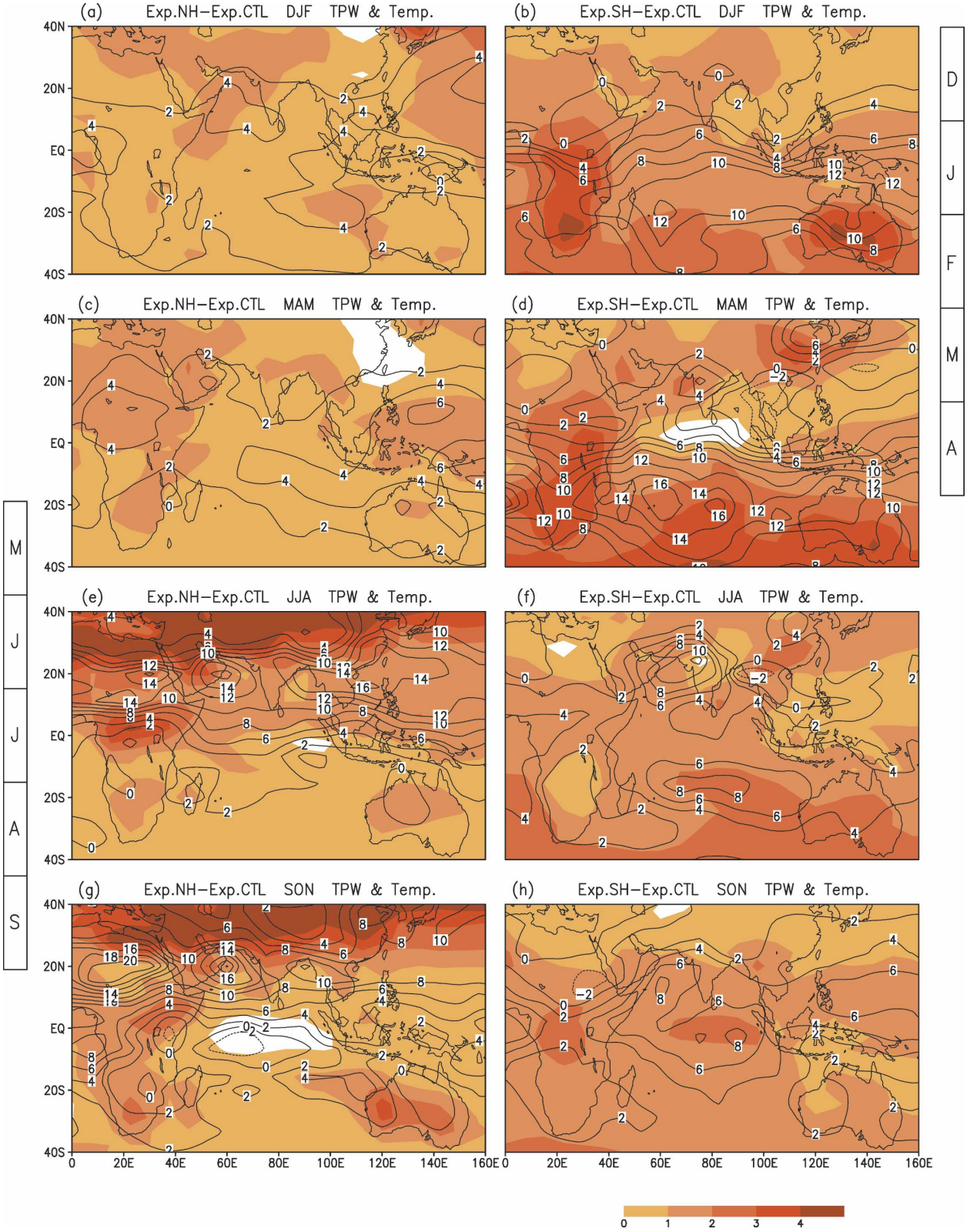

FIG. 4. (left) Seasonally averaged TPW (contour, mm) and surface temperature (shaded, °C) differences between experiments NH and CTL and (right) those between experiments SH and CTL for (a), (b) DJF, (c), (d) MAM, (e), (f) JJA, and (g), (h) SON. Only positive differences in surface temperature are shown here. The left (right) column indicates the months during which insolation is increased in the NH (SH) in experiment NH (SH).

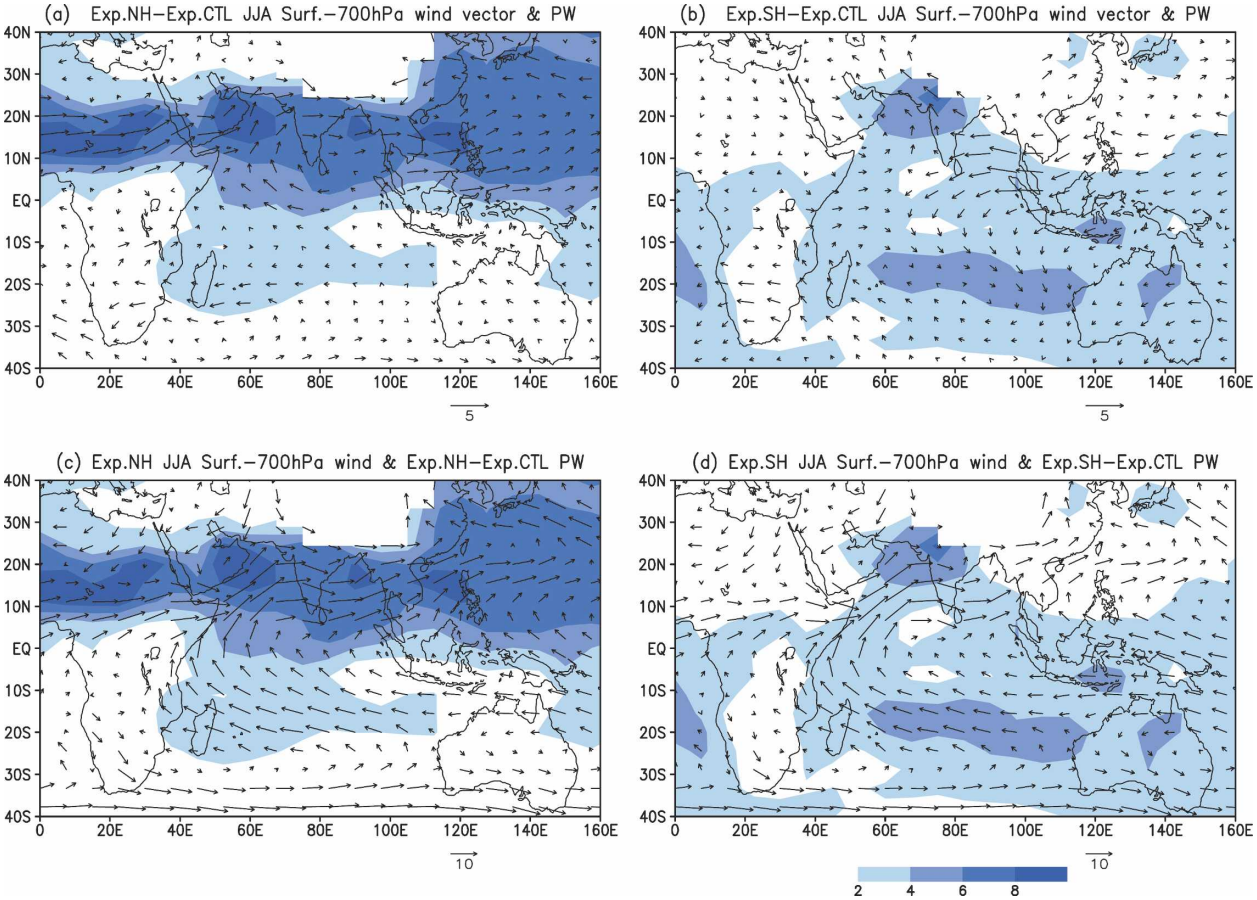

FIG. 5. (a) JJA surface–700-hPa mass-weighted mean wind vector (m s^{-1}) difference and precipitable water (PW; mm) difference between experiments NH and CTL. Only positive PW differences are shown. (b) Same as in (a), but for difference between experiments SH and CTL; (c) JJA surface–700-hPa mass-weighted mean wind vector in experiment NH and PW difference between experiments NH and CTL. Only positive differences are shown. (d) Same as in (c), but for mean wind vector in experiment SH and PW difference between experiments SH and CTL.

closely associated with the variability of the Asian monsoon (Singh et al. 2000). TPW, which is defined as the total water vapor obtained by integrating the mass-weighted specific humidity vertically from the surface to the top of an atmospheric column, varies evidently with hemispheric insolation changes in our experiments (Fig. 4). In comparison with the control run, the NH insolation increase produces more TPW in the boreal Tropics from North Africa to East Asia in JJA and SON (Figs. 4e and 4g). The SH insolation increase results in more TPW over the southern Indian Ocean, Africa, and Australia. When the SH insolation is enhanced from December to April, the largest increase in TPW occurs in the southern Indian Ocean in MAM, (Fig. 4d). The patterns of TPW change are consistent with those of the SST change. Therefore, the increased SST is responsible, in large part, for the increase of TPW in the southern Indian Ocean.

c. *Lower-tropospheric wind*

The surplus or deficiency of the North African and South Asian monsoon rainfall at an orbital scale is usually related to monsoon circulation strength (Kutzbach 1981; Braconnot et al. 2002). Hence, the change in monsoonal circulation must be examined in order to understand the increase in precipitation with enhanced hemispheric insolation. The JJA lower-tropospheric wind vector difference between experiments NH and CTL shows that the southwesterly wind is much stronger in experiment NH than that in experiment CTL over the Arabian Sea and across northern Africa (Fig. 5a). The JJA lower-tropospheric wind vector difference between experiments SH and CTL is small over the Arabian Sea, although westerly and southerly wind components are slightly enhanced (Fig. 5b). The southwesterly winds over the Bay of Bengal weaken in experiment SH

compared with that in experiment CTL, resulting in an anomalous convergence over India.

At the same time, we also examined changes of precipitable water in the lower troposphere below 700 hPa (Fig. 5). In the following we abbreviate the surface–700-hPa vertically integrated water vapor (i.e., precipitable water) to PW to differentiate it from TPW. Actually, spatiotemporal variations of PW are similar to those of TPW (not shown). Our result demonstrates that the intensive NH summer insolation induces more PW in the northern Tropics from North Africa to South and East Asia (Fig. 5a). Similarly, enhanced SH insolation in boreal winter and spring gives rise to increased PW over the Arabian Sea, India, and the southern tropical Indian Ocean in boreal summer (Fig. 5b). We note that the change in the PW pattern is, to a certain extent, consistent with change in the circulation field as shown in experiment NH minus experiment CTL. That is, the regions with increased PW generally coincide with those of enhanced winds (Fig. 5a). However, the increased PW seems not directly linked to changed winds in experiment SH minus experiment CTL (Fig. 5b). On the other hand, the pattern of PW difference between experiments SH and CTL corresponds well with the pattern of mean circulation in experiment SH (Fig. 5d). Two centers of the PW difference are located over the central-eastern tropical Indian Ocean and the northern Arabian Sea–northwestern Indian peninsula. These results strongly suggest that the mean airflow, perhaps slightly enhanced by the flow from the SH forcing, is responsible for the increase of PW over the northern Arabian Sea–northwestern Indian peninsula in experiment SH. This observation indicates that summer mean cross-equatorial flow along the east coast of Africa, over western Indian Ocean, transports the increased PW from the southern tropical Indian Ocean to the northern Arabian Sea, bringing about more PW and eventually more precipitation in parts of South Asia.

d. Moisture flux

To further evaluate moisture transport from the SH to the NH, we focus on the horizontal moisture flux in this section. The JJA surface–700-hPa vertically integrated moisture flux vector and its divergence (Fig. 6) display intensive moisture transport from the southern tropical Indian Ocean to South Asia and strong moisture convergence (i.e., negative divergence) over South Asia in the control case (Fig. 6a). In comparison with experiment CTL, enhanced moisture convergence, accompanying stronger westerly moisture transport along the equator and stronger inflow to North Africa and South and East Asia, arises in JJA in experiment NH (Fig. 6b). In contrast to experiment NH is experiment

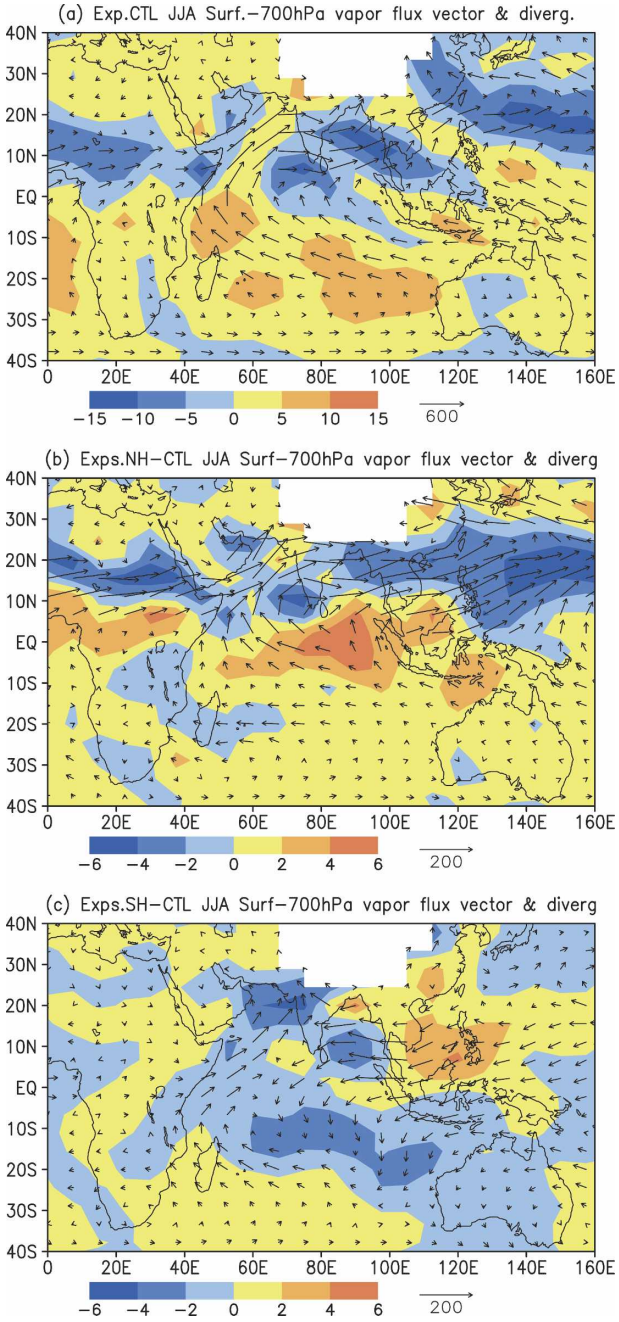

FIG. 6. JJA moisture flux vector (kg m^{-1} s) and its divergence (10^{-5} kg m^{-2} s^{-1}), integrated vertically from the surface to 700 hPa, for experiments (a) CTL, (b) NH minus CTL, and (c) SH minus CTL.

SH, which exhibits considerable interhemispheric moisture transport (Fig. 6c). A moisture transport belt along the east coast of Africa links a center of anomalous moisture convergence over the southern Indian Ocean to the moisture convergence center over western South Asia (Fig. 6c), consistent with the patterns of JJA mean circulation and especially the anomaly PW field in ex-

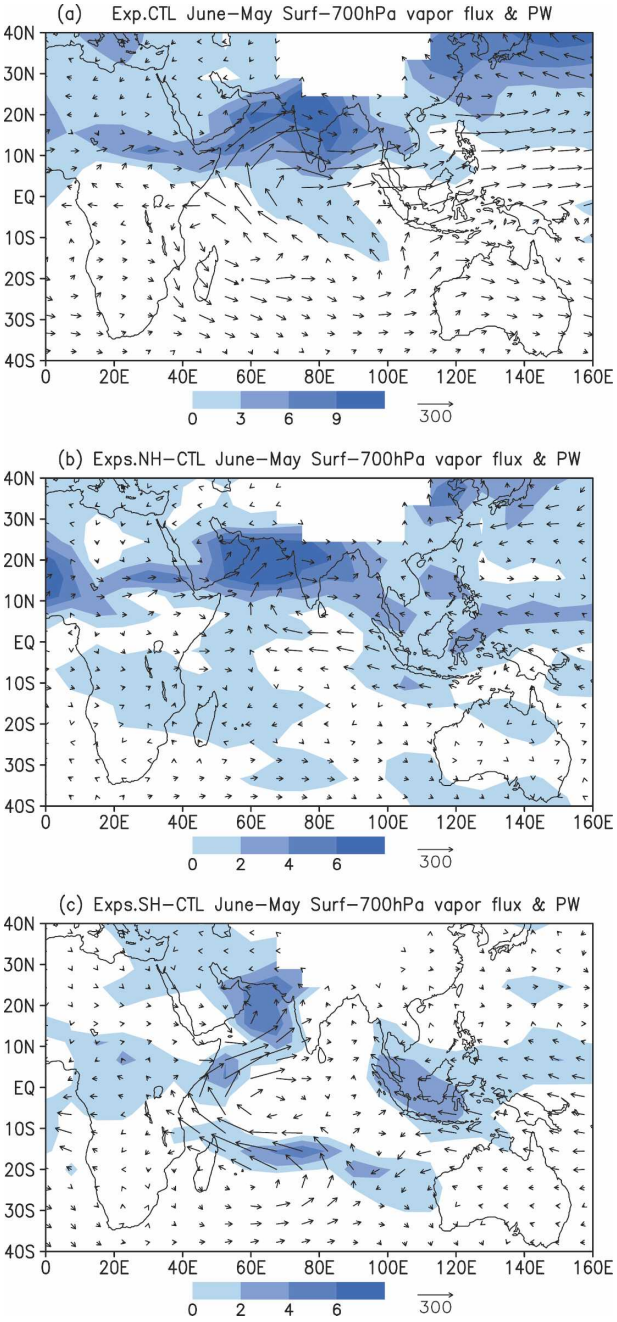

FIG. 7. Differences of surface–700-hPa moisture flux vector (kg m^{-1} s) and PW (mm) between June and May in experiment (a) CTL; (b) NH minus CTL; (c) SH minus CTL. Only positive PW differences are shown.

periment SH (Fig. 5d). This shows again that increased SH insolation from December to April reinforces the boreal summer moisture export to parts of South Asia from the southern Indian Ocean.

The enhanced interhemispheric moisture transport is most distinct during the transition season with the onset of the Asian monsoon. As shown in Fig. 7a, both the surface–700-hPa moisture flux from the SH and PW over South Asia increase distinctly from May to June with the monsoon onset in the control simulation. Although the PW over the Arabian Sea in boreal summer is increased in both experiment NH (Fig. 7b) and in experiment SH (Fig. 7c) in comparison with experiment CTL; only in experiment SH is the lower-tropospheric water vapor transport crossing the equator off the African coast strengthened from May to June (Fig. 7c). It follows that the increased PW or TPW over the Arabian Sea with the onset of the Asian monsoon does result from the enhanced moisture source in the southern tropical Indian Ocean when the SH insolation forcing is intensified.

e. Asymmetry

The Indian Ocean and Asian monsoon are affected by both the remote and the local insolation forcing. However, the responses of precipitation over the Indian Ocean and Asian monsoon region to SH and NH insolation changes are asymmetric, as shown below. The maxima of globally zonally averaged JJA and January–March (JFM) precipitation occur at 7°–16°N and 11°–20°S (Fig. 8a), but at 7°–11°N and 7°–11°S for the 60°–100°E average (Fig. 8b) in experiment CTL. Globally, precipitation obviously increases at 11°–20°N for JJA when NH insolation is strengthened from May to September (Fig. 8c), while the greatest increase of precipitation is found at 16°–20°S for JFM when SH insolation is reinforced from December to April (Fig. 8e). In other words, hemispheric insolation intensification induces increased global-scale precipitation in the same hemisphere and in the same season, exhibiting a kind of local forcing. Hence, the response of the global zonal mean precipitation to hemispheric insolation forcing is roughly symmetrical. However, the response of the zonal mean precipitation in the monsoon sector (60°–100°E) to SH and NH hemispheric insolation changes is highly asymmetric. As contrasted with experiment NH, in which the major increase in precipitation appears at about 24°N over South Asia in JJA (Fig. 8d), the increased precipitation in experiment SH occurs both at 16°S in JFM and at 24°N in JJA in response to enhanced SH insolation from December to April (Fig. 8f). This indicates that the preceding SH insolation has a remote and delayed influence on the South Asian summer monsoon (Fig. 8f). An asymmetric response in the sense that the corresponding cross-hemisphere delayed response in the NH experiment is very small (Fig. 8d). In addition, from Fig. 8d (Fig. 8f) we note that the JJA (DJF) precipitation decreases

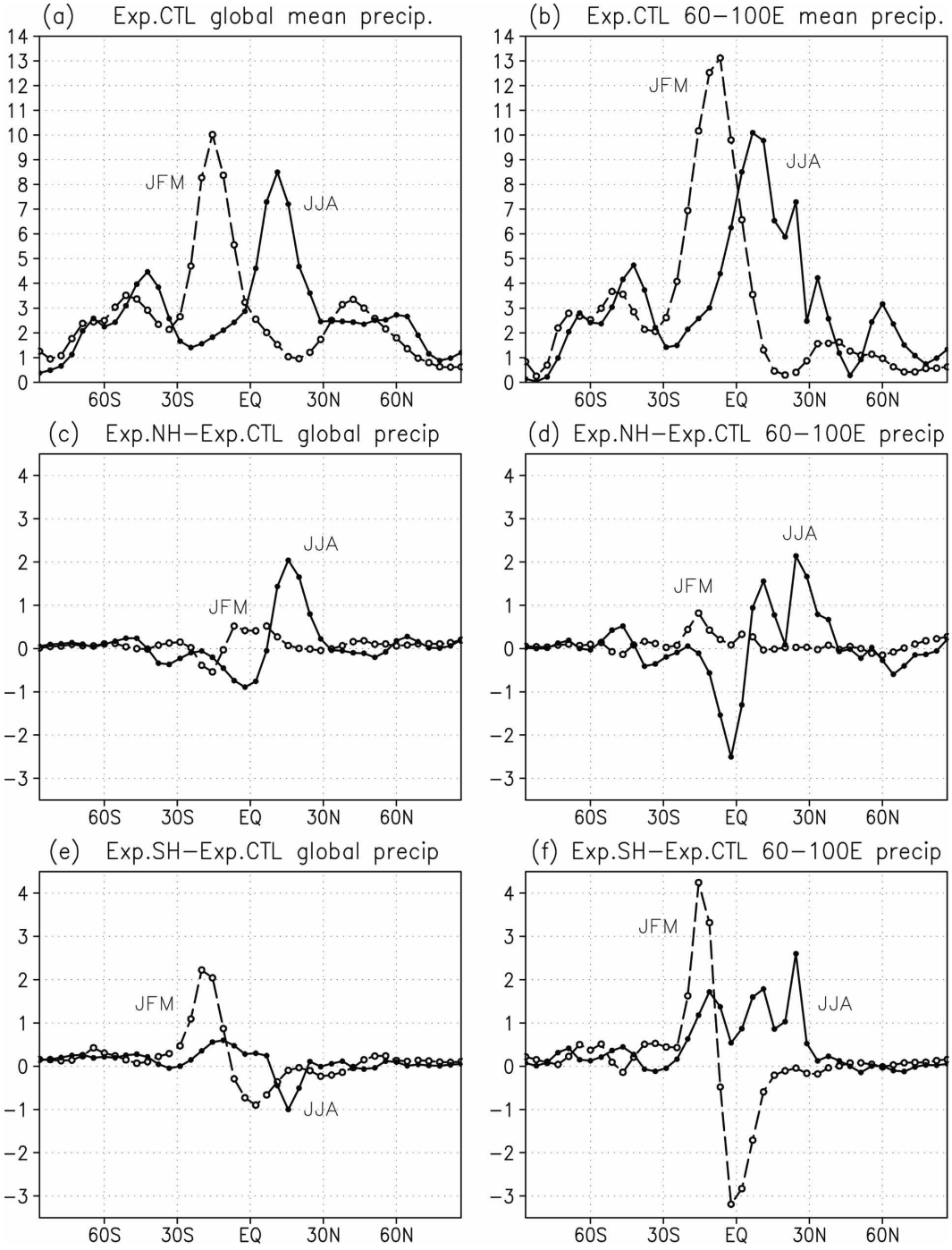

FIG. 8. JJA (solid lines) and JFM (dashed lines) precipitation rate (mm day^{-1}) averaged zonally (left) around the globe and (right) for the longitudinal band of 60°–100°E in experiment (a), (b) CTL, (c), (d) NH minus CTL, and (e), (f) SH minus CTL.

over the equatorial Indian Ocean in experiment NH (experiment SH), which is related to a northward (southward) shift of the intertropical convergence zone (ITCZ) as a direct response to the hemispheric insolation increase.

4. Summary and discussion

We have shown that the NH and SH insolation changes both affect the Indian Ocean and Asian monsoon. Comparing the NH and SH insolation influences,

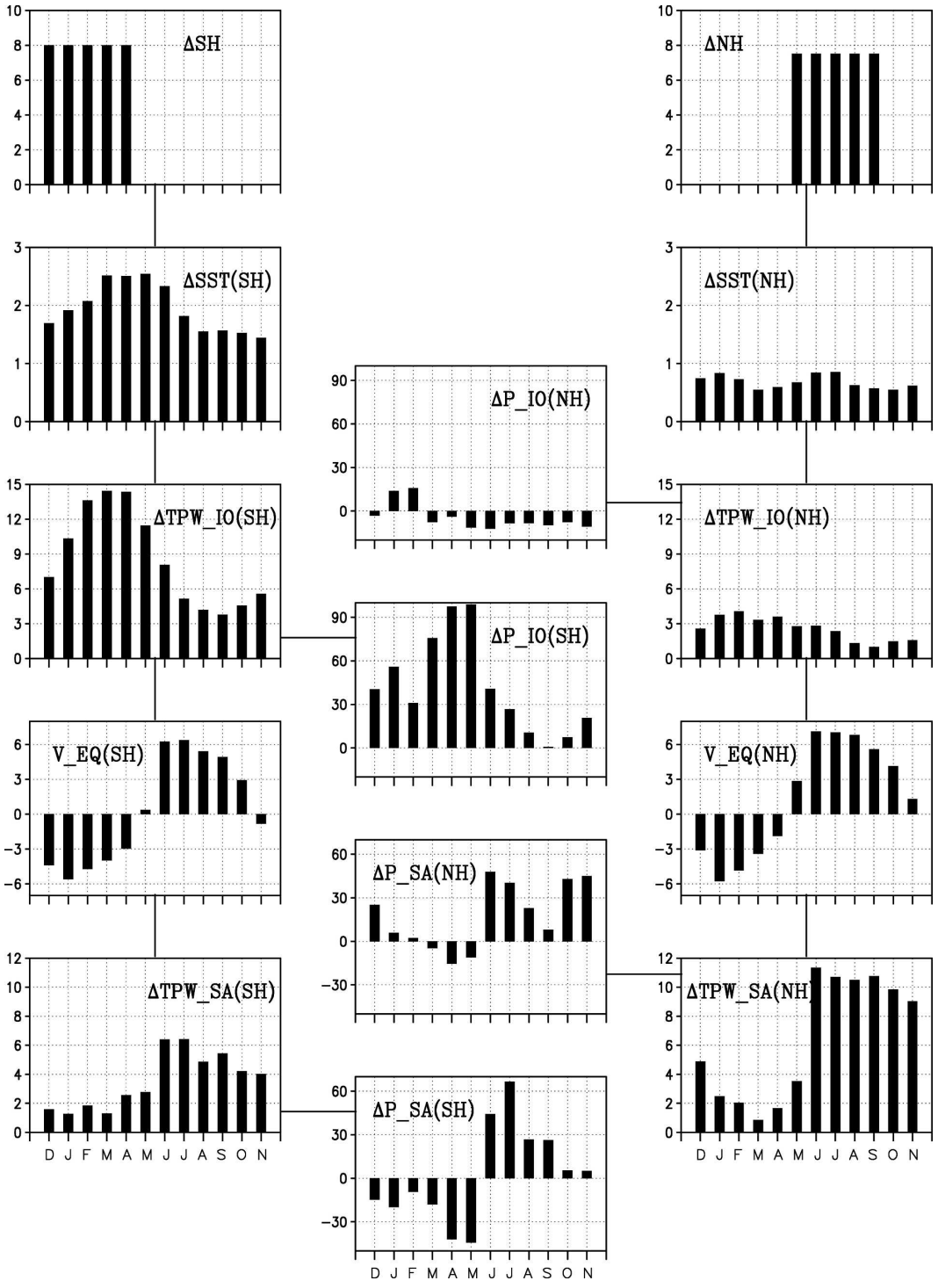

FIG. 9. Summary of hemispheric insolation influences on the Indian Ocean and South Asian monsoon. The parameter ΔSH (ΔNH) indicates the percentage change of monthly SH (NH) insolation in experiment SH (NH) compared with that in CTL; ΔSST, ΔTPW_IO, and ΔP_IO represent the monthly changes of SST, TPW, and precipitation in the southern tropical Indian Ocean (5°–30°S, 55°–95°E), respectively; ΔTPW_SA and ΔP_SA are TPW over western South Asia (5°–30°N, 50°–90°E) and precipitation over western South Asia (5°–30°N, 60°–100°E; Land and Ocean), respectively. The "SH" ("NH") in parentheses means experiment SH (NH) minus CTL; V_EQ(SH) and V_EQ(NH) indicate the surface–700-hPa mass-weighted mean meridional wind speed averaged for 40°–70°E at the equator in experiments SH and NH, respectively.

our results indicate that the NH insolation change has a local and immediate impact on the NH summer monsoons from North Africa to Asia while the SH insolation change has a remote and delayed effect on the South Asian summer monsoon rainfall. The hemispheric insolation influence on the Indian Ocean and South Asian monsoon is summarized in Fig. 9. As indicated in the left panels, when SH insolation is increased by 8% from December to April compared with the control run (see ΔSH in Fig. 9), the SST in the southern tropical Indian Ocean (5°–30°S, 55°–95°E) rises between 1° and 3°C [see ΔSST(SH)], especially during January to July. The increased SST can bring about more TPW over the southern tropical Indian Ocean [see ΔTPW_IO(SH)] by promoting evaporation, and enhancing local precipitation in MAM [see ΔP_IO(SH)]. Meanwhile, the lower-tropospheric meridional wind over the western equatorial Indian Ocean (40°–70°E) changes from northerly to southerly with the onset of the South Asian monsoon mean circulation [see V_EQ(SH)]. As a result, the increased TPW over the Indian Ocean is transported northward to the monsoon region, increasing the TPW over western South Asia (5°–30°N, 50°–90°E) [i.e., ΔTPW_SA(SH)], and eventually leading to increased summer precipitation over western South Asia (5°–30°N, 60°–100°E; Land and Ocean) [see ΔP_SA(SH)]. The right panels in Fig. 9 show that the increase of 7.5% in the NH insolation (ΔNH) from May to September fails to induce a significant response in SST or TPW in the southern tropical Indian Ocean [see ΔSST(NH) or ΔTPW_IO(NH)] but directly strengthens the South Asian TPW and precipitation during June to November [see ΔTPW_SA(NH) and ΔP_SA(NH), respectively] through local forcing.

One important finding of this work related to the SH indirect forcing is that the increased TPW over the southern tropical Indian Ocean and corresponding increased low-troposphere moisture transport from the southern tropical Indian Ocean toward South Asia is associated with the climatological mean winds rather than strengthened winds. The simulated increase in precipitation supports, in part, the hypothesis that latent heat forcing from the southern tropical Indian Ocean plays a role in setting the phase of the Indian monsoon at the precession and obliquity bands as inferred from the geological record (Clemens et al. 1991; Clemens and Prell 2003). However, the model response to both NH and SH forcing and inferences from the geological record need further checking for several reasons. Most importantly, these experiments used idealized insolation changes and did not include the full seasonal cycle and the full latitudinal distribution of insolation found in orbital forcing. Experiments with full orbital forcing and higher-resolution models may help to confirm our overall findings and also help connect our results more clearly to proxy records from particular localities.

The model results indicating increased precipitation without significantly increased circulation are more or less similar to those forecast for global warming conditions (increased atmospheric CO_2) as reported in previous modeling studies. Increased Asian monsoon precipitation has been ascribed to warmer Indian Ocean SSTs in the future climate being able to supply an enhanced moisture source to fuel stronger monsoon rainfall. Therefore, the response of the monsoon rainfall is not solely related to the changes in the large-scale dynamics, rather, changes in atmospheric moisture play an important role in the precipitation response. For example, Kitoh et al. (1997) reported increased monsoon rainfall in their transient climate change simulation without any increase in the strength of the monsoon circulation and suggested that the increase in monsoon rainfall could arise in response to increased atmospheric moisture in a warmer climate. Douville et al. (2000) found that an increase in atmospheric water content can increase monsoon precipitation despite weakening of the monsoon flow in a warmer climate. Meehl and Arblaster (2003) predicted that the intensification of monsoon rainfall associated with greenhouse warming is related to a nonlinear enhancement of moisture source from the warmer Indian Ocean. Ashrit et al. (2003) showed that the increase in monsoon precipitation is partly due to a "nondynamical" response to global warming, namely a large increase in precipitable water over India, but does not show a clear strengthening of monsoon circulation. Recently, May's (2004) time slice experiment also predicts an intensification of Indian summer rainfall associated with enhanced atmospheric moisture transport into the monsoon region due to the general warming, while the future changes in the large-scale flow indicate a weakening of monsoon circulation in the upper troposphere and only little change in the lower troposphere.

Another interesting result here is a clear interhemispheric asymmetry in precipitation response to SH and NH insolation forcing. The intensified NH insolation during May to September heightens boreal summer rainfall over North Africa and South and East Asia and has little influence on SH and other season's precipitation. However, enhanced SH insolation during December to April increases precipitation not only over the southern Indian Ocean in MAM but also over western South Asia in JJA. Why is there this asymmetry between the SH and NH? First, there exists a large asymmetry in land–sea geometry. Examining land–sea dis-

tribution between 40°S and 40°N from 40° to 120°E, one can see that the northern portion is mainly covered by land while the southern portion is occupied almost entirely by ocean. As a result, intensified NH insolation mainly heats the northern landmass (see Figs. 4e,g), thus causing little SH effect since the thermal storage is limited and the atmospheric and oceanic circulation is insufficient to export the signal. On the other hand, the stronger SH insolation in boreal winter and early spring heats the southern Indian Ocean locally (see Figs. 4b,d) but does influence the subsequent Indian summer monsoon through a comparatively longer memory and interhemispheric ocean–atmospheric circulation as Prasad et al. (2000) suggested. Second, the summer monsoon is much stronger than the winter monsoon over South Asia (Wang et al. 2003a). Therefore, the lower-tropospheric northward flow in boreal summer greatly exceeds the southward flow in boreal winter over the eastern tropical Indian Ocean, facilitating the SH influence on the NH.

The overall goal of our work is to investigate the impact of the SH insolation change induced by the orbital forcing on the variability of the Asian summer monsoon. However, this initial experiment used idealized insolation forcing rather than orbital insolation forcing. Our results from these idealized experiments identify one process by which SH summer insolation forcing can influence NH summer precipitation in India, but do not take into account the full seasonal and latitudinal features of orbitally caused insolation changes, nor do they explore relationships with terrestrial ice volume. Moreover, whereas the modeling results attribute the increased Indian monsoon rainfall to greater PW but not increased lower-troposphere circulation, the geologic data mostly reflect strengthened surface winds and oceanic upwelling related to the SH forcing. Causes of these remaining inconsistencies need to be studies. In our future work, we need also to more fully quantify the relative importance of local versus remote insolation forcing and the superposed moisture transport effect and further explore the role of glacial boundary conditions in determining the timing and strength of the South Asian monsoon. We note that Tuenter et al. (2005) recently performed a set of long transient simulations with a coupled model of intermediate complexity to explore millennial-scale climate phase lags in response to precession and obliquity forcing. Ultimately, as computer resources permit, we will conduct multimillennial simulations with fully coupled ocean–atmospheric models in an effort to better resolve mechanisms linking forcing to the monsoon response.

Acknowledgments. All numerical experiments were completed on the supercomputer at the National Center for Atmospheric Research. The National Center for Atmospheric Research is sponsored by the National Science Foundation. This work was jointly supported by NSF grants to Brown University (OCE-0352215) and to the University of Wisconsin—Madison (OCE-0352362), China's "973" Program (2004CB720208), and NSFC (40472086). We also acknowledge the support of the University of Wisconsin—Madison and the NSF through their joint support of Chinese National Academy of Science collaboration with the University of Wisconsin—Madison. Xiaodong Liu was a Visiting Scientist at the University of Wisconsin—Madison during a portion of this research work.

REFERENCES

Ashrit, R. G., H. Douville, and K. R. Kumar, 2003: Response of the Indian monsoon and ENSO-monsoon teleconnection to enhanced greenhouse effect in the CNRM Coupled Model. *J. Meteor. Soc. Japan,* **81,** 779–803.

Berger, A., and M. F. Loutre, 1991: Insolation values for the climate of the last 10 million years. *Quat. Sci. Rev.,* **10,** 297–317.

Braconnot, P., O. Marti, S. Joussaume, and Y. Leclainche, 2000: Ocean feedback in response to 6 kyr BP insolation. *J. Climate,* **13,** 1537–1553.

——, M. F. Loutre, B. Dong, S. Joussaume, P. Valdes, and PMIP Participating Groups, 2002: How the simulated change in monsoon at 6 ka BP is related to the simulation of the modern climate: Results from the Paleoclimate Modeling Intercomparison Project. *Climate Dyn.,* **19,** 107–121.

Clemens, S. C., 1999: An astronomical tuning strategy for Pliocene sections: Implications for global-scale correlation and phase relationships. *Philos. Trans. Roy. Soc. London,* **357A,** 1949–1973.

——, and R. J. Oglesby, 1992: Interhemispheric moisture transport in the Indian Ocean summer monsoon: Data-model and model-model comparisons. *Paleoceanography,* **7,** 633–643.

——, and W. L. Prell, 2003: A 350 000 year summer-monsoon multi-proxy stack from the Owen Ridge, Northern Arabian Sea. *Mar. Geol.,* **201,** 35–51.

——, ——, D. W. Murray, G. Shimmield, and G. Weedon, 1991: Forcing mechanisms of the Indian Ocean monsoon. *Nature,* **353,** 720–725.

——, D. W. Murray, and W. L. Prell, 1996: Nonstationary phase of the Plio-Pleistocene Asian Monsoon. *Science,* **274,** 943–948.

de Noblet, N., P. Braconnot, S. Joussaume, and V. Masson, 1996: Sensitivity of simulated Asian and African summer monsoons to orbitally induced variations in insolation 126, 115 and 6 kBP. *Climate Dyn.,* **12,** 589–603.

Ding, Z., Z. Yu, N. Rutter, and T. S. Liu, 1994: Towards an orbital time scale for Chinese loess deposits. *Quat. Sci. Rev.,* **13,** 39–70.

Douville, H., J. F. Royer, J. Polcher, P. Cox, N. Gedney, D. B. Stephenson, and P. J. Valdes, 2000: Impact of CO_2 doubling on the Asian summer monsoon: robust versus model-dependent responses. *J. Meteor. Soc. Japan,* **78,** 421–439.

Gallimore, R., J. E. Kutzbach, and R. L. Jacob, 2005: Coupled

atmosphere-ocean-vegetation simulations for modern and mid-Holocene climates: Role of extratropical vegetation cover feedbacks. *Climate Dyn.,* **25,** 755–776.

Hewitt, C. D., and J. F. B. Mitchell, 1998: A fully coupled GCM simulation of the climate of the mid-Holocene. *Geophys. Res. Lett.,* **25,** 361–364.

Imbrie, J., and Coauthors, 1992: On the structure and origin of major glaciation cycles: 1. Linear responses to Milankovitch forcing. *Paleoceanography,* **7,** 701–738.

Jacob, R., 1997: Low frequency variability in a simulated atmosphere ocean system. Ph.D. thesis, University of Wisconsin—Madison, 155 pp.

Khodri, M., Y. Leclainche, G. Ramstein, P. Braconnot, O. Marti, and E. Cortijo, 2001: Simulating the amplification of orbital forcing by ocean feedbacks in the last glaciation. *Nature,* **410,** 570–574.

Kitoh, A., S. Yukimoto, A. Noda, and T. Motoi, 1997: Simulated changes in the Asian summer monsoon at times of increased atmospheric CO_2. *J. Meteor. Soc. Japan,* **75,** 1019–1031.

Kudrass, H. R., A. Hofmann, H. Doose, K. Emeis, and H. Erlenkeuser, 2001: Modulation and amplification of climatic changes in the Northern Hemisphere by the Indian summer monsoon during the past 80 k.y. *Geology,* **29,** 63–66.

Kutzbach, J. E., 1981: Monsoon climate of the Early Holocene: Climate experiment with the Earth's orbital parameters for 9000 years ago. *Science,* **214,** 59–61.

——, and P. Guetter, 1986: The influence of changing orbital parameters and surface boundary conditions on climate simulations for the past 18 000 years. *J. Atmos. Sci.,* **43,** 1726–1759.

——, and Z. Liu, 1997: Response of the African monsoon to orbital forcing and ocean feedbacks in the middle Holocene. *Science,* **278,** 440–443.

Leuschner, D. C., and F. Sirocko, 2003: Orbital insolation forcing of the Indian Monsoon—A motor for global climate changes? *Palaeogeogr. Palaeoclimatol. Palaeoecol.,* **197,** 83–95.

Liu, T. S., Z. L. Ding, and N. Rutter, 1999: Comparison of Milankovitch periods between continental loess and deep sea records over the last 2.5 Ma. *Quat. Sci. Rev.,* **18,** 1205–1212.

Liu, Z., and L. Wu, 2004: Atmospheric response to the North Pacific SST: The role of ocean–atmosphere coupling. *J. Climate,* **17,** 1859–1882.

——, J. Kutzbach, and L. Wu, 2000: Modeling climatic shift of El Nino variability in the Holocene. *Geophys. Res. Lett.,* **27,** 2265–2268.

——, S. P. Harrison, J. Kutzbach, and B. Otto-Bliesner, 2004: Global monsoons in the mid-Holocene and oceanic feedback. *Climate Dyn.,* **22,** 157–182.

May, W., 2004: Potential future changes in the Indian summer monsoon due to greenhouse warming: Analysis of mechanisms in a global time-slice experiment. *Climate Dyn.,* **22,** 389–414.

Meehl, G. A., 1997: The south Asian monsoon and the tropospheric biennial oscillation. *J. Climate,* **10,** 1921–1943.

——, and J. M. Arblaster, 2002: GCM sensitivity experiments for the Indian monsoon and tropospheric biennial oscillation transition conditions. *J. Climate,* **15,** 923–944.

——, and ——, 2003: Mechanisms for projected future changes in South Asian monsoon precipitation. *Climate Dyn.,* **21,** 659–675.

Morley, J. J., and L. E. Heusser, 1997: Role of orbital forcing in east Asian monsoon climates during the last 350 kyr: Evidence from terrestrial and marine climate proxies from core RC14-99. *Paleoceanography,* **12,** 483–494.

Philander, S. G., and A. V. Fedorov, 2003: Role of tropics in changing the response to Milankovitch forcing some three million years ago. *Paleoceanography,* **18,** 1045, doi:10.1029/2002PA000837.

Prasad, K. D., S. D. Bansod, and S. S. Sabade, 2000: Forecasting Indian summer monsoon rainfall by outgoing longwave radiation over the Indian Ocean. *Int. J. Climatol.,* **20,** 105–114.

Prell, W. L., 1984: Monsoonal climate of the Arabian Sea during the Late Quaternary: A response to changing solar radiation. *Milankovitch and Climate,* A. L. Berger et al., Eds., D. Riedel, 349–366.

——, and E. Van Campo, 1986: Coherent response of Arabian Sea upwelling and pollen transport to late Quaternary monsoonal winds. *Nature,* **323,** 526–528.

——, and J. E. Kutzbach, 1987: Monsoon variability over the past 150 000 years. *J. Geophys. Res.,* **92,** 8411–8425.

Rind, D., 2002: The Sun's role in climate variations. *Science,* **296,** 673–677.

Ruddiman, W. F., 2001: *Earth's Climate: Past and Future*. W. H. Freeman & Sons, 465 pp.

Singh, R. P., N. C. Mishra, A. Verma, and J. Ramaprasad, 2000: Total precipitable water over the Arabian Ocean and the Bay of Bengal using SSM/I data. *Int. J. Remote Sens.,* **21,** 2497–2503.

Sitch, S., and Coauthors, 2003: Evaluation of ecosystem dynamics, plant geography and terrestrial carbon cycling in the LPJ dynamic global vegetation model. *Global Change Biol.,* **9,** 161–185.

Tuenter, E., S. L. Weber, F. J. Hilgen, L. J. Lourens, and A. Ganopolski, 2005: Simulation of climate phase lags in response to precession and obliquity forcing and the role of vegetation. *Climate Dyn.,* **24,** 279–295.

Wajsowicz, R. C., and P. S. Schopf, 2001: Oceanic influences on the seasonal cycle in evaporation over the Indian Ocean. *J. Climate,* **14,** 1199–1226.

Wang, B., S. Clemens, and P. Liu, 2003a: Contrasting the Indian and East Asian monsoons: Implications on geologic time scale. *Mar. Geol.,* **201,** 5–21.

——, R. Wu, and T. Li, 2003b: Atmosphere–warm ocean interaction and its impacts on Asian–Australian monsoon variation. *J. Climate,* **16,** 1195–1211.

Wehausen, R., and H.-J. Brumsack, 2002: Astronomical forcing of the East Asian monsoon mirrored by the composition of Pliocene South China Sea sediments. *Earth Planet. Sci. Lett.,* **201,** 621–636.

Wu, L., and Z. Liu, 2003: Decadal variability in the North Pacific: The eastern North Pacific mode. *J. Climate,* **16,** 3111–3131.

——, and ——, 2005: North Atlantic decadal variability: Air–sea coupling, oceanic memory, and potential Northern Hemisphere resonance. *J. Climate,* **18,** 331–349.

Zhu, Y. L., and D. D. Houghton, 1996: The impact of Indian Ocean SST on the large-scale Asian summer monsoon and the hydrological cycle. *Int. J. Climatol.,* **16,** 617–632.